

p-band stability of ultracold atom gas in anharmonic optical lattice potential with large energy scales

Mateusz Łącki

Institute of Theoretical Physics, Jagiellonian University, Łojasiewicza 11, 30-348 Kraków, Poland

Using an optical potential with subwavelength resolution in the form of sharp δ -like peaks, potential landscapes are created with increased anharmonicity in placement of lattice band energies and more favorable energy scales. In particular, this makes the ultracold atom *p*-band gas more stable. The article outlines the details of the construction and discusses the *p*-band stability in canonical cosine optical lattice potential, double well potential, and a combination of a classical cosine potential with dark state peaked potential.

I. INTRODUCTION

Optical lattices make a convenient and powerful setting for experimental study of many-body physics using ultracold atoms. An observation that such systems are described by Hubbard-type models [1], followed by a realization of the Mott insulator-superfluid quantum phase transition [2], led to numerous proposals and experiments with ultracold atoms [3].

One of the research directions was populating higher bands of optical lattices [4, 5] with the ongoing debate on stability of such systems. This was in part motivated by prospects to create interesting superfluid states, time reversal symmetry breaking [6, 7] or emergence of $p_x + ip_y$ order [8, 9], or quantum Hall physics [10, 11].

In addition to theory proposals, questions of more practical significance have been raised – a problem of preparing gas in the excited bands [12–15] and the question of stability and lifetime of such a gas [4, 16–18].

Higher bands can also be populated by coherent resonant band coupling [12–14, 19]. When the coupling of *s* to *p* band is resonant, and presence of other bands can be disregarded, a synthetic-dimension two-leg ladder system, carrying flux π per ladder plaquette is created [20].

In the standard optical lattice, the collisional stability of the *p*-band e.g. is limited due to the fact that total energy of two particles in *p* band is often very close to the configuration where one particle is in *s* and the other in the *d* band. This process is off-resonant when the lattice band energies are anharmonic, leading to prolonged lifetime, as observed in the experiment [4, 21, 22].

Deviation from equal spacing between subsequent band *s, p, d, ...*, necessary for collisional *p*-band stability has to dominate other energy scales such as interaction strength or amplitudes of time-dependent fields. The latter can be lowered, thus increasing the stability. The price to pay however would be limits on simulable physics, given practical limits on coherence time of ultracold lattice systems. The real solution should be in the direction of making energy levels in lattice systems more anharmonic, and the energy scales larger.

In [23, 24] a method of creating a potential in the form of a comb of subwavelength, few-nanometer wide peaks was proposed. It carries bands with non-harmonic energies $\sim n^2$. Moreover subwavelength-width double well

systems [25] allow large values of energy scales for hopping and interaction.

In this work we explore the effects the anharmonic level spacing has on collisional stability of *p*-band gas and on coherent resonant coupling of *s* and *p* bands. We also study the energy scales for the parameters of tight-binding models describing motion of ultracold atom in such potentials.

In Section II we review the tight-binding description of an ultracold atom gas in few lowest Bloch bands of the optical potential. We discuss energy level arrangement for various particular potentials: “standard” \cos^2 optical lattice, the double well lattice, subwavelength comb potential, and a combination of comb potential and the standard \cos^2 lattice. In Section III we discuss the simulation of long-term depletion of the *p*-band by collisional interactions in case for all considered optical potentials. In Section IV, we study the creation of the synthetic-dimension two-leg ladder system in *s* and *p* band of a 1D lattice system, focusing on the achieved energy scales and the containment of the system. We provide summary and outlook in Section V.

II. MULTIBAND DESCRIPTION OF THE ULTRACOLD ATOM GAS IN THE OPTICAL LATTICES

The gas of ultracold atoms of mass m_a in the periodic optical potential $V_{\text{opt.}}(r)$ is canonically described by the second quantization Hamiltonian of the form [1]:

$$H_X = \int d^3r \hat{\psi}^\dagger(r) \left[-\frac{\hbar^2}{2m_a} \nabla^2 + V_{\text{opt.}}(r) \right] \hat{\psi}(r) + \frac{g}{2} \int \hat{\psi}^\dagger(r) \hat{\psi}^\dagger(r) \hat{\psi}(r) \hat{\psi}(r) d^3r. \quad (1)$$

The $g = \frac{4\pi a_s \hbar^2}{m_a}$ is the strength of two-particle collisional interactions by *s*-wave scattering with a scattering length a_s , tunable by Feshbach resonances [26]. Tight harmonic confinement $m_a \Omega^2 (y^2 + z^2)/2$ in *y* and *z* makes the system effectively 1D.

The rest of this Section is organized as follows. In the Subsection II A we restate the multiband tight-binding

description of (1). In Subsection II B we briefly introduce the four potentials that will be compared for the p -band stability using the quantity f which is introduced in the second part of this Subsection. In Subsections II C-II F we discuss the particular quantitative features of the four potentials considered in this work.

A. Tight-binding description

In this section we recapitulate the conventional multi-band tight-binding description of the Hamiltonian (1).

The x -periodic potential, $V_{\text{opt.}}(\vec{r}) = V_{\text{opt.}}(x) + m_a \Omega^2 (y^2 + z^2)/2$ admits a family of x -quasiperiodic eigenfunctions $B_k^\alpha(\vec{r}) = B_k^\alpha(x) \mathcal{H}(y) \mathcal{H}(z)$, $B_k^\alpha(x+a) = B_k^\alpha(x) e^{ika/\hbar}$ for each band $\alpha = 0, 1, 2, \dots$ (with $\alpha = 1$ corresponding to the p band) to the eigenenergy $E^\alpha(k)$. The k is a quasimomentum taken from the Brillouin zone $k \in [-\pi/a, \pi/a]$, a is the lattice constant, and $\mathcal{H}(\cdot)$ is the harmonic potential ground state. For large enough Ω just the lowest mode in y, z is populated which reduces down to global energy shift. In this work we consider only $V_{\text{opt.}}(x)$ which are smooth and have one or two minima in one period.

For isolated bands, for each lattice site x_n , exponentially localized Wannier functions $W_n^\alpha(x)$ can be constructed under mild assumptions [27–29]. Specifically:

$$W_n^\alpha(x) = N \int_{k \in BZ} B_k^\alpha(x) e^{i(\theta_k + kan)} dk,$$

where θ_k is chosen to minimize the spatial variance of the Wannier functions, and N ensures unit L^2 norm of W_n^α 's [27–29].

When the Hamiltonian (1) is expressed in the basis $W_k^\alpha(x)$, the Multi-band Bose-Hubbard (MBH) Hamiltonian is obtained

$$H_{\text{MBH}} = - \sum_{\alpha, n, m} J_{nm}^{\alpha\alpha} (\hat{a}_n^\alpha)^\dagger \hat{a}_m^\alpha + H.c. + \frac{1}{2} \sum_{\substack{\alpha \dots \delta \\ n \dots p}} U_{nmop}^{\alpha\beta\gamma\delta} (\hat{a}_n^\alpha)^\dagger (\hat{a}_m^\beta)^\dagger \hat{a}_o^\gamma \hat{a}_p^\delta, \quad (2)$$

where:

$$J_{nm}^{\alpha\alpha} = - \int dx W_n^\alpha(x) \left(-\frac{\hbar^2}{2m} \nabla^2 + V_{\text{opt.}}(x) \right) W_m^\alpha(x) \\ = \frac{1}{\text{vol}(BZ)} \int_{BZ} e^{i(n-m)ka} E^\alpha(k) dk, \quad (4)$$

and

$$U_{nmop}^{\alpha\beta\gamma\delta} = g \int d\vec{r} W_n^\alpha(\vec{r}) W_m^\beta(\vec{r}) W_o^\gamma(\vec{r}) W_p^\delta(\vec{r}). \quad (5)$$

In particular, $J_{nn}^{\alpha\alpha} \equiv \bar{E}_n^\alpha$ is the on-site energy of a particle at site n and band α . The $J_{n, n+1}^{\alpha\alpha} \equiv J^\alpha$ is nearest-neighbor hopping rate within band α . In the formula

for integrals $U_{nmop}^{\alpha\beta\gamma\delta}$, an integral of $H^4(y)H^4(z)$ over y, z directions gives an overall factor that is incorporated in g .

When the gas populates the p -band, the full model (2) reduces to a single band Bose-Hubbard model,

$$H_{BH} = -J \sum_{\langle n, m \rangle} (\hat{a}_n^\dagger \hat{a}_m + H.c.) + \sum_m \frac{U}{2} \hat{n}_m (\hat{n}_m - 1), \quad (6)$$

where $U = U_{nnnn}^{1111}$, $J = J_{n, n+1}^{11} = J^1$. The model exhibits superfluid-Mott insulator quantum phase transition which occurs for $J/U \approx 0.3$ [2, 30–34]. The question of whether the multi-band model H_{MBH} can be truncated to single band H_{BH} is the central question of this paper.

The Hamiltonian H_{MBH} describes a complex many-body system which is non-integrable. It conserves the total number of particles. Conventionally the truncation of the total Hilbert space is by restricting the H_{MBH} to lowest few bands. The Hilbert space for H_{MBH} for gas of N particles occupying L site lattice within lowest α_{max} bands has dimension $\binom{N + \alpha_{\text{max}} L - 1}{N}$ which is a prohibitively large number of parameters for representing the Hamiltonian or even eigenvectors for large systems.

Efficient numerical simulation is not possible in lattices in dimension higher than 1. The dynamics of the single-band variant, the Bose-Hubbard model can be effectively simulated in the 1D lattices using the TEBD or various tensor network approaches. Time-complexity of these methods is proportional to the $\sim d^3$ where d is the single-site Hilbert space dimension. For $\alpha_{\text{max}} = 3$, and truncation at 6 particles per lattice site, we have $d = 10$, factor $O(10)$ larger than “typical” cutoffs for BH Hamiltonian calculations. Ultimately the limit of application of these methods for simulation of the dynamics is growth of entanglement entropies.

In this work, to minimize the computational effort, we restrict our study to small systems of density $N/L > 1$, and to minimize the boundary effects, periodic boundary conditions are used. For $L = 6$ and $\alpha_{\text{max}} = 3$ the full representation of vectors can be used.

B. Optical potentials and p -band collisional stability

This section provides a short overview of different optical potentials considered in this work. In the second part we introduce quantity f which is useful for quantifying p -band stability of these potentials.

For ultracold atoms arbitrary optical potentials can be created using either stroboscopic projection schemes (as proposed in [35]) or spatial light modulators (as exemplified in [36–38]). Such techniques, however, imply either short system lifetime or relatively long lattice constants $a \gg \lambda/2$ and in turn overall low energy scale for lattice dynamics given by the recoil energy $E_R = \frac{\hbar^2}{8ma^2}$. The reliable workhorse for ultracold lattice systems have

been potentials due to the AC-Stark shift from a laser standing-wave, far detuned from an optical transition [1]:

$$V_{\text{latt}}(x) = V_x \cos^2 kx, \quad k = 2\pi/\lambda \quad (7)$$

where λ is the laser wavelength. By using two laser wavelengths the following potential is obtained [39]:

$$V_{dw}(x) = V_2 \cos^2(k_2 x) + V_1 \cos^2(k_1 x + \phi), \quad k_1 = \frac{k_2}{2}. \quad (8)$$

The above potential has been prominently used in $V_2 > V_1/4$ regime, where it features two minima per period. It is of main interest for us for $V_2 = V_1/4$ where it is a lattice potential with unique minimum per period, which is quartic.

Recently a scheme, based on coherent dark-state of atomic Λ system has been proposed [23, 24] that allows to create comb potentials of the form:

$$V_{na}(\epsilon, x) = E_R \frac{\epsilon^2 \cos^2 kx}{(\epsilon^2 + \sin^2 kx)^2}, \quad (9)$$

where $\epsilon \ll 1$ [see also Fig.3(a)].

The fourth class considered in this work is the combined potential

$$V_{\text{comb}}(x) = V_{na}(x) + V_{\text{latt}}(x). \quad (10)$$

All the above potentials share a common feature that the unit cell contains one or two potential minima (as detailed in Sections II C-II F). Then the low lying bands s, p, d, \dots are *generally* simple, single-valued bands separated by a nonzero gap. The Wannier functions corresponding to different bands spatially overlap. The notable exception is the double well potential in the regime when it has two very deep potential wells per period. In this work we are interested however in the case when s and p band spatially overlap.

For a ultracold gas in the lattice p -band, a possible loss mechanism is when collisions push particles to different bands: one to s -band and one to the d -band. This process may be (nearly) resonant, when the wells of $V_{\text{opt}}(x)$ are well approximated by a harmonic potential.

Let us consider two weakly-interacting particles in the p -band with energy in the interval $\mathcal{A} = [2 \min E^1(q), 2 \max E^1(q)]$ and collisional population of the final state with energy in $\mathcal{B} = [\min E^0(q) + \min E^2(q), \max E^0(q) + \max E^2(q)]$. The process $p + p \rightarrow s + d$ is not resonant only if the distance between intervals \mathcal{A} and \mathcal{B} is much larger than the interaction-induced coupling, namely when

$$f \equiv \text{dist}(\mathcal{A}, \mathcal{B}) \approx |2\bar{E}^1 - \bar{E}^0 - \bar{E}^2| - 2|2|J^1| + |J^0| + |J^2|| \gg U_{nnnn}^{1120}. \quad (11)$$

The ratio f/U_{nnnn}^{1120} thus quantifies the extent to which the description of p -band gas given by Eq. (6) is valid. At the same time one desires that the parameters U, J

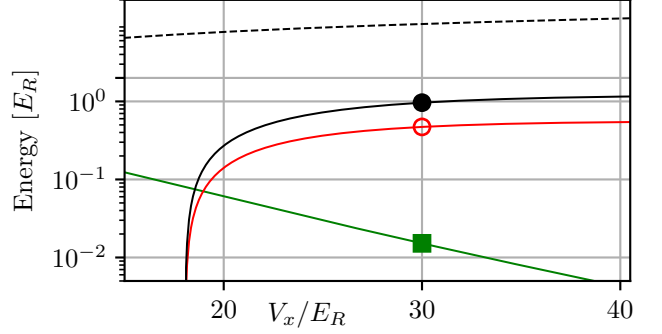


Figure 1. Figure shows the value of f (black curve, marked with full circle), Δ_{sp} (black dashed line), and U^{1111} (red solid line, marked with empty circle) assuming $U^{1120} = f/10$, J^1 (green curve, marked with a full square), for the classical optical potential V_{latt} as the function of its height V_x – see Eq. (7).

in Eq. (6) are as large as possible in the absolute terms to make the system stable against thermal fluctuation. Additionally the time-scales defined by the model should be within coherence time of possible experimental setups.

In the forthcoming Sections we show the calculation of the parameter f of the four potentials Eq.(7)-(10). We also remind the familiar relevant energy scales for hopping, interaction and band separation for the four potentials.

C. Standard optical lattice potential

The low-energy sector of a Hamiltonian [Eq. (1)] describing a particle in the lattice potential $V_{\text{latt}}(x)$ [Eq. (7)] for $V_x \gg E_R$ resembles a system with a series of almost-decoupled nearly-harmonic traps. Taking into account quartic terms in expansion of \cos^2 potential around its minima gives an approximate formula for n -th band energy:

$$E_n \approx \left(n + \frac{1}{2}\right) \sqrt{4V_x E_R} - E_{qu}, \quad E_{qu} = \frac{6n^2 + 6n + 3}{12} E_R. \quad (12)$$

The above expression is frequently used when truncated to just the first term $\sim \sqrt{V_x}$. While it is often sufficient, we note that in $V_x \rightarrow \infty$ limit the quartic contribution E_{qu} is non-vanishing. The f defined in Eq. (11) for very large $V_x \gg E_R$, when all the hopping rates J^0, J^1, J^2 are exponentially suppressed is therefore:

$$f \approx 2E_1 - E_0 - E_2 \rightarrow 1E_R \quad (13)$$

It is important to stress that the limit value in Eq. (13) is nonzero solely due to the quartic term in Eq.(12).

Specifically the f is nonzero [see Fig. 1] for $V_x \gtrsim 18E_R$. At around $V_x \approx 30E_R$, f reaches $1E_R$. The maximum value of f is attained near $V_x \approx 40E_R$ where $f \approx 1.4E_R$.

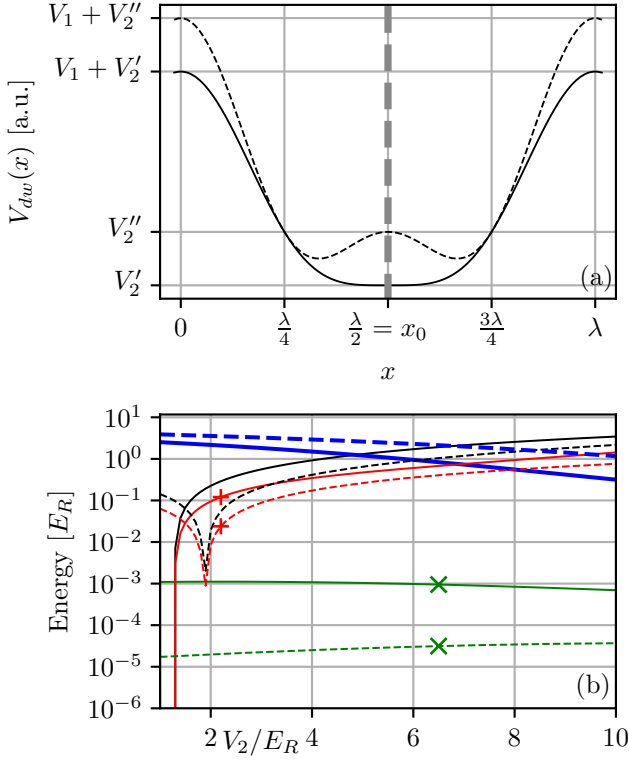


Figure 2. Figure shows the properties of the potential V_{dw} . Panel (a) parallels the discussion of the potential shape and symmetry in the main text; the vertical dashed gray line shows the symmetry axis. Solid line shows V_{dw} for $V_2 = V_2' = V_1/4$. Dashed line shows $V_2 = V_2'' = V_1/2$ case. Panel (b) shows the value of f (black curve), Δ_{sp} (blue, thick line), and U^{1111} (red with a '+'), J^1 (green with a 'x') assuming $U^{1120} = f/10$, for the two-well optical potential V_{dw} as the function of V_2 with $V_1 = 10E_R$ (solid lines) or $V_1 = 20E_R$ (dashed lines). See Eq. (8).

Increasing the lattice height V_x and therefore f comes at the price of decrease of J^1 . For $V_x \approx 30E_R$ ($40E_R$) we have $J^1 \approx 0.015E_R$ ($0.0042E_R$).

These p -band hopping rates are quite small. For a popular atom species used often in experiments, the ^{87}Rb , typical parameters of lasers, the hopping frequency would be of the order of few tens of Hertz.

D. “Double-well” potential

By using two lasers one can create, by an AC-Stark shift a potential of the form (8). It has been used in countless theoretical and experimental works (just a few examples being [39–43]).

The double-well potential V_{dw} has a fundamental period twice larger than $V_{\text{latt}}(x)$, namely $a = \lambda$. When $\phi = 0$ the potential is symmetric with respect to the center of the properly chosen unit cell x_0 [see Fig. 2(a)]. The Wannier functions of $s, p, d \dots$ band are then alternately even and odd with respect to the x_0 . For $V_2 \leq V_1/4$ the poten-

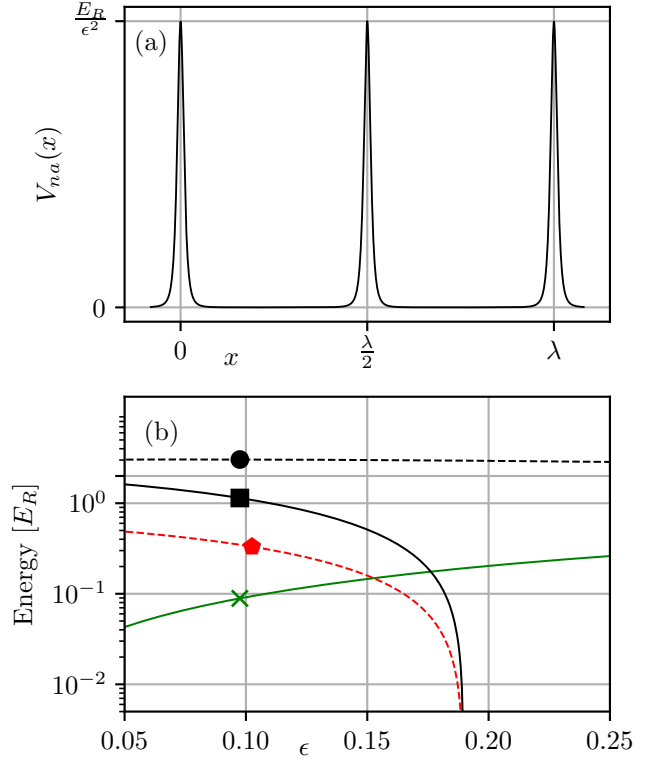


Figure 3. Figure shows the properties of the potential V_{na} . Panel (a) presents the shape and height of a potential V_{na} parametrized by ϵ . Panel (b) shows the value of f (black curve with a square), Δ_{sp} (black dashed line with a circle), and U^{1111} (red dashed line with a pentagon), J^1 (green with a cross) assuming $U^{1120} = f/10$, for the comb optical potential V_{na} as the function dimensionless parameter ϵ – see Eq. (9).

tial remains unimodal within the unit cell with minimum at x_0 . At exactly $V_1 = V_2/4$ at $\partial_{xx}V_{dw}(x_{\min}) = 0$, and the potential around the minimum is well-approximated by a quartic potential [see Fig. 2(a)]. For larger V_2 there are two minima and the s to p band gap is significantly reduced.

The Fig. 2(b) shows the dependence of factor f as a function of V_2 for fixed $V_1 = 10E_R$ (solid lines) and $V_1 = 20E_R$ (dashed lines). We see that for $V_2 \approx V_1/4$ the factor f is $0.35E_R$ for $V_1 = 10E_R$ and $f \approx 0.65E_R$ for $V_2 = 20E_R$ the values of f reached are not larger than those achievable for the standard optical lattice ($f \leq 1.4E_R$). This is primarily due to twice larger period of the unit cell. As a result the increased anharmonicity due to the dominant quartic term is scaled down by factor 4, $E'_R = \frac{\hbar^2}{8ma^2} = \frac{E_R}{4}$, $a = \lambda$. The value of f can be increased by increasing both V_1 and V_2 . For fixed $V_2 = V_1/4$, in the limit of very large V_1, V_2 the factor f can be arbitrarily large (in contrast to the V_{latt}). The price to pay is the exponential decay of J^1 , which for $V_1 = 10E_R$ is $O(10^{-3}E_R)$ and for $V_1 = 20E_R$ is $O(10^{-5} \div 10^{-4}E_R)$. Increasing just V_2 , while formally leading to the increase of f , actually leads to the degeneration of p and s band.

E. Comb potential

In this section we review in detail the construction of the comb potential (the presentation follows [23]) with a particular focus on the parameters ϵ and x_0 which control the height and the position of the potential peak. The details of the construction are then referred to in discussion of V_{comb} in the Subsection II F.

The potential $V_{na}(x)$ as given by Eq. (9) transpires in the three level system [23]:

$$H_c = -\frac{\hbar^2}{2m_a}\partial_x^2 + H_\Lambda(x), \quad (14)$$

where

$$H_\Lambda(x) = \hbar \begin{pmatrix} 0 & \Omega_c(x)/2 & 0 \\ \Omega_c(x)/2 & -\Delta - i\Gamma/2 & \Omega_p/2 \\ 0 & \Omega_p/2 & 0 \end{pmatrix} \quad (15)$$

has been written in the atomic level basis $|g_1\rangle, |e\rangle, |g_2\rangle$. The Rabi frequency $\Omega_c(x)$ is a standing wave,

$$\Omega_c(x) = \Omega_c \sin[k(x - x_0)], \quad (16)$$

and Ω_p is x -independent,

$$\epsilon = \frac{\Omega_p}{\Omega_c}. \quad (17)$$

The position-dependent eigenstates of $H_\Lambda(x)$ include the dark state $|f_1(x)\rangle = -\cos\alpha(x)|g_1\rangle + \sin\alpha(x)|g_2\rangle$ with $\alpha(x) = \arctan[\Omega_c(x)/\Omega_p]$. It is an eigenstate to the zero energy for all x .

The Hamiltonian H_c is well approximated by the following Hamiltonian (with V_{na} given by Eq. 9):

$$H_{na} = -\frac{\hbar^2}{2m_a}\partial_x^2 + V_{na}(x), \quad (18)$$

when it acts on wavefunctions of the form $\psi_D(x) = g(x)|f_1(x)\rangle$ of low energy $\langle\psi_D|H_{na}|\psi_D\rangle$.

The potential V_{na} has the form of sharp potential peaks [see 3(a)] of height E_R/ϵ^2 and width $\sim \epsilon\lambda/2\pi$, located at $x = n\lambda/2 + x_0, n \in \mathbb{Z}$.

When $\epsilon \rightarrow 0$ the potential peaks can be replaced by $\frac{\pi}{2\epsilon} \sum_n \delta(x - x_0 - n\lambda/2)$. In that limit, mean band energies converge to values characteristic for a box potential, $E_n \approx n^2 E_R$. It may be shown that the bandwidths of each band $\Delta E_n \approx 4J^n \sim n^2 \epsilon E_R$ [see [23]].

The potential V_{na} allows to reach similar values of f as the standard optical lattice V_{latt} ($f \approx 1.4E_R$ for $\epsilon = 0.05$, and $f \approx 1E_R$ for $\epsilon = 0.1$) [see Fig. 3(b)]. The anharmonicity of the mean band energies is $|2\bar{E}_p - \bar{E}_s - \bar{E}_d| \approx 2E_R$ but only for very small $\epsilon \approx 0$, the hopping J^0, J^1, J^2 is suppressed. Experiments conducted to this date operated with values of $\epsilon \geq 0.05$ [24, 44]. Further reduction would necessitate using strong lasers creating the Ω_c, Ω_p

which would couple the system beyond three levels included in (15). Use of atoms with trivial hyperfine structure would be a possible solution to the issues raised with first experiments. It should be also noted that the above Λ system has not been so far experimentally realized with the bosonic species.

The values of hopping amplitude J^1 for $\epsilon \geq 0.05$ are actually order of magnitude larger than J^1 for V_{latt} for same value of f ($J^1 \approx 0.09E_R$ for $\epsilon = 0.1$, and for $\epsilon = 0.05$ it is $J^1 \approx 0.042E_R$). In contrast to V_{latt} it is challenging to significantly reduce J^1 as the potential barrier height $\sim \epsilon^{-2}$ increased with ϵ is partially compensated by its decreasing width $\sim \epsilon$. In the subwavelength comb the s to p and s to d band separations are almost ϵ -independent and $\Delta_{sp} \approx 3E_R, \Delta_{pd} \approx 5E_R$.

F. Classical potential together with the comb potential

Another possibility is opened by a combined potential that includes both a standard lattice potential V_{latt} and the V_{na} potential (parameter ϕ allows for shift of V_{na} peak with respect to the minimum of V_{latt}) [25]:

$$V_{\text{comb}}(x) = V_{\text{latt}}(x) + V_{na}(\epsilon, x - a\phi), \quad a = \lambda/2 \quad (19)$$

The combined potential $V_{\text{comb}}(x)$ can be achieved when in Eq. (15) atoms in either of states g_1 and g_2 feel an additional, standard lattice potential due to AC-Stark shift, namely when the three-level Hamiltonian is of the form [24].

$$H_\Lambda(z) = \hbar \begin{pmatrix} V_1 \sin^2(kx) & \Omega_c(x - a\phi)/2 & 0 \\ \Omega_c(x - a\phi)/2 & -\Delta - i\Gamma/2 & \Omega_p/2 \\ 0 & \Omega_p/2 & V_1 \sin^2(kx) \end{pmatrix}.$$

The potential $V_1 \sin^2(kx)$ is then simply added to $V_{na}(x - a\phi)$ resulting in the desired $V_{\text{comb}}(x)$.

In the pure $V_{\text{latt}}(x)$ potential the Wannier functions are alternately even and odd w.r.t to the center of the unit cell. A sharp potential in the middle of the cell, would primarily shift energies of each band, by a value $\int_{\mathbb{R}} V_{na}(x)|W^\alpha(x)|^2 dx \approx \pi|W(0)|^2/(2\epsilon)$. The integral is maximal for the s -band Wannier functions, and decays for subsequent even Wannier functions. It is zero for odd bands, including the p -band. As the anharmonicity, for deep lattice is given by $f \approx 2\bar{E}^1 - \bar{E}^0 - \bar{E}^2 > 0$, adding the central V_{na} peak should first lower the f first towards zero. Only after that the f can attain, large negative values.

Non-central placement of the $V_{na}(\epsilon, x)$ offers more flexibility in manipulating the $f \approx 2\bar{E}^1 - \bar{E}^0 - \bar{E}^2$ (see also [25]). For example, when the subwavelength peaks V_{na} coincide with maxima of the p -band Wannier function of $V_{\text{latt}}(x)$ one can expect the mean \bar{E}^1 to increase strongly in contrast to \bar{E}^0 and \bar{E}^2 . As a result the band anharmonicity should be increased to large positive values.

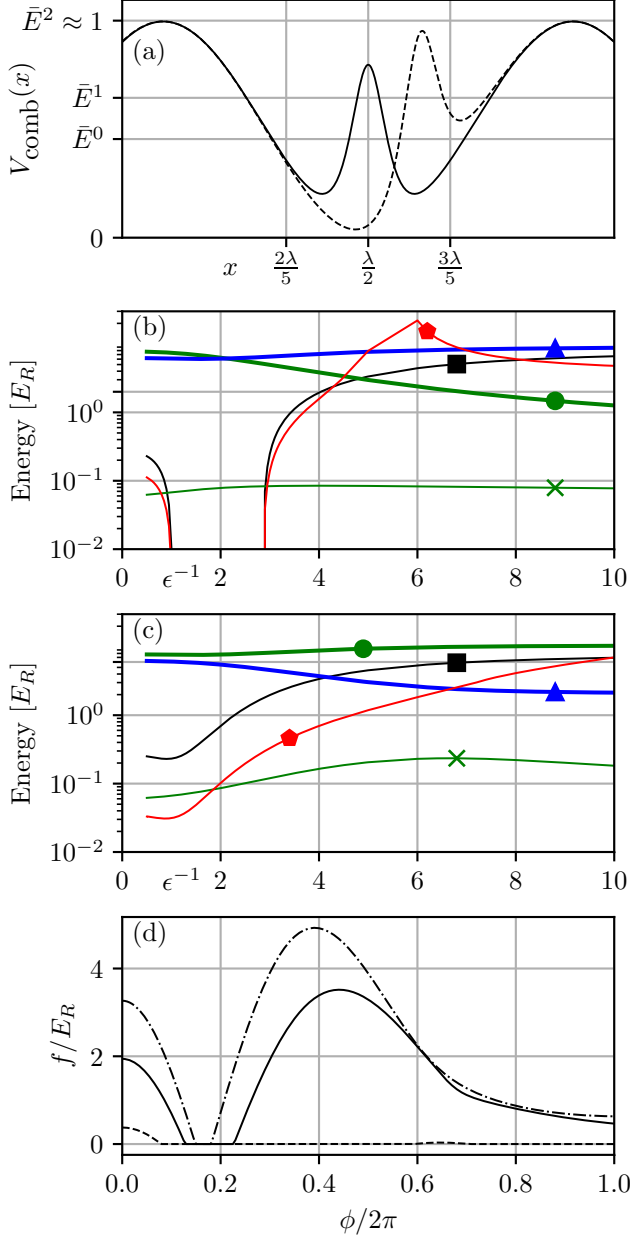


Figure 4. Properties of V_{comb} . Panel (a) shows the potential shape, around the potential minimum for $V_x = 20E_R$, $\epsilon = 0.25$ and $\phi = 0$ (black solid line), $\phi = 0.4/\pi$ (black dashed line). The levels $\bar{E}^0, \bar{E}^1, \bar{E}^2$ indicate first three band energies for $\phi = 0$. Panels (b) and (c) show the value of f (black curve with a square), Δ_{sp} (green, thick line with a filled circle), Δ_{pd} (blue, with a triangle pointing up), and U^{1111} (red with a pentagon), J^1 (green with a cross) assuming $U^{1120} = f/10$, for the combined optical potential V_{comb} (comb potential and classical \sin^2 potential) as the function of dimensionless parameter ϵ controlling the height of the comb potential with $V_x = 20E_R$, $\phi = 0$ [panel (b)] or $V_x = 20E_R$, $\phi = 0.4/2\pi$ [panel (c)]. See Eq. (8). Panel (d) shows f/E_R for $V_x = 10, 20, 30E_R$ and $\epsilon^{-1} = 4$ (dashed, solid, dash-dotted black line) as a function of a shift ϕ of subwavelength peak w.r.t to the potential minimum.

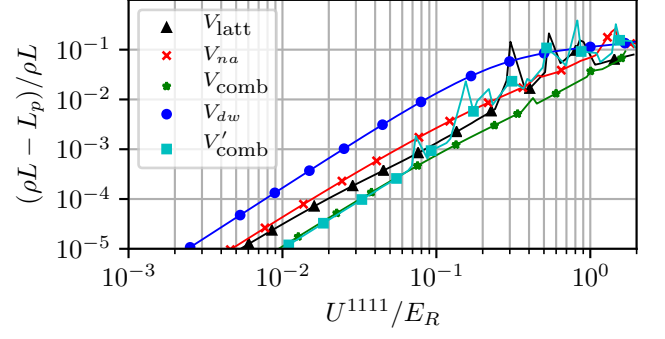


Figure 5. Mean losses from the p -band population of an interacting system for the four considered potentials, in a system of length $L = 6$ populated with $\rho L = 7$ particles. The exact parameters are given by Eqs. (20)-(24).

In Fig. 4(a) shows the parameters describing the properties of the V_{comb} for $\phi = 0$ and for $\phi = 0.4/\pi$. In the latter case $V_{na}(x - a\phi)$ nearly coincides with maximum of the p -band Wannier function.

When $\phi = 0$ it is evident that the values of f that easily achieve value of $f = 2E_R$ (for $\epsilon \approx 0.25$) before, for even smaller ϵ , the central peak given by V_{na} cuts the potential well into two almost disconnected parts, with tiny Δ_{sp} . For $\phi = 0$ we focus on $\epsilon \approx 0.25$ when the \bar{E}^1 is similar to the V_{na} peak height, the Wannier function of the p band is not strongly affected by the potential peak and Δ_{sp} remains sizable.

For small ϵ^{-1} the potential V_{comb} can resemble the potential V_{dw} . The crucial difference is that its period remains $a = \lambda/2$ in contrast to period λ of V_{dw} . This allows to maintain much higher hopping rate in V_{comb} .

When $\phi = 0.4/\pi$ the values of f that are reached are similar, with important difference: the value of $f = 2\bar{E}^1 - \bar{E}^0 - \bar{E}^2$ for $\epsilon^{-1} \rightarrow 0$ does not change the sign as ϵ^{-1} is increased. This means that in contrast to $\phi = 0$, also for $\epsilon^{-1} \leq 3$ the f is nonzero. This is important for practical applications as the spontaneous emission losses quickly grow with ϵ^{-1} (see [23, 24]).

For all considered ϕ the hopping rate $J^1 \approx 0.1 \div 0.15E_R$. It is half of the order of magnitude larger than for V_{latt} of the same potential height. This is simply due to the fact that putting extra potential V_{na} in the potential well makes it effectively shallower. In contrast to using a standard optical lattice V_{latt} working with the value of $f \approx 1 - 2E_R$ requires $V_x = 15 \div 20E_R$ while for V_{latt} the $f \approx 1 - 1.4E_R$ is reached for deep lattices of $V_x = 30 \div 40E_R$ with J^1 hopping rate significantly reduced. At such value of ϵ the combined potential retains workable features of the V_{latt} such as sizable $\Delta_{sp} \approx 3.8E_R$.

III. COLLISIONAL STABILITY OF P-BAND CONDENSATE

In this section we numerically study the stability of the p -band gas in the potentials from the previous Section II. To this end we consider a small, strongly interacting system consisting of $L = 6$ sites described by Hamiltonian H_{MBH} in Eq. (2) under periodic boundary conditions, restricted to lowest three bands, $\alpha_{\text{max}} = 3$.

1. Potential V_{latt} of height $V_x = 30E_R$ with $f \approx 1E_R$ and:

$$(J^0, J^1, u, u') \approx (-0.00046E_R, 0.015E_R, 0.698, 4.89), \quad (20)$$

2. Potential V_{na} for $\epsilon = 0.1$ with $f \approx 1.11E_R$ and:

$$(J^0, J^1, u, u') \approx (-0.022E_R, 0.091E_R, 0.985, 3.05), \quad (21)$$

3. Potential V_{comb} of $V_2 = 20E_R$, $\epsilon = 0.25$, $\phi = 0$ with $f \approx 1.94E_R$ and:

$$(J^0, J^1, u, u') \approx (-0.024E_R, 0.084E_R, 0.933, 9.02), \quad (22)$$

4. Potential V_{comb} of $V_2 = 20E_R$, $\epsilon = 0.25$, $\phi = 0.4/2\pi$ with $f \approx 3.38E_R$ and:

$$(J^0, J^1, u, u') \approx (-0.00074E_R, 0.11E_R, 0.445, 5.88), \quad (23)$$

5. Potential V_{dw} of $V_1 = 20E_R$, $V_2 = 4E_R$ with $f \approx 0.65E_R$ and:

$$(J^0, J^1, u, u') \approx (-1.16 \times 10^{-6}E_R, 2.5 \times 10^{-5}E_R, 0.802, 4.00). \quad (24)$$

Initially the quantum state of the gas of $N_p = \rho L$ particles is an eigenstate ψ_0 of the Hamiltonian H_{MBH} , Eq. (2) with no interactions, $g = 0$. The chosen initial state is the least energy eigenstate where all the particles populate the p -band – it is a product of Bloch functions with quasimomentum $q = q_*$ minimizing $E^1(q)$.

The subsequent evolution $\psi(t) = \exp(-iH_{\text{MBH}}t/\hbar)\psi_0$ is governed by full H_{MBH} truncated to lowest three bands, $\alpha < \alpha_{\text{max}} = 3$. The population of the p -band is given by

$$N_p(t) = \langle \psi(t) | \hat{n}_p | \psi(t) \rangle$$

Initially, $N_p(t = 0) = \rho L$. For $t > 0$ the population $N_p(t)$ drops due to interaction-driven coupling to other bands. The temporal dependence shows some long-term oscillatory behavior that is attributed to the finiteness of the system and that of the Hilbert space. To mitigate these effects, we consider a long-time average $L_p = \overline{N_p(t)}$.

Let us discuss the dependence of $N_p(t)$ and L_p on the interaction strength g , that can be altered by means of a Feshbach resonance [26].

The value of $\xi = J^1/U^{1111}$ parameter together with ρ indicate the position in the phase diagram of the BH

model. The absolute value of J^1 [Eqs. (20)-(24)] is however smaller by V_{latt} of V_{dw} by order of magnitude or more than V_{na} or V_{comb} . To ensure that all four cases correspond to the same quantum phase – superfluid state, we fix the system density to $\rho = 7/6 > 1$. As a result all the four systems have essentially the same probability for double occupation of the lattice site.

Under such assumptions the relative loss defined as $\delta = (\rho L - L_p)/\rho L$ measures the depletion of the p -band. As revealed by a numerical simulation, for as long as $U^{1111} \ll f$ the losses δ for potentials $V_{\text{latt}}, V_{na}, V_{\text{comb}}, V_{dw}$ scale as $\delta = A(U^{1111}/E_R)^\alpha$. Fitting the numerical data show in Fig. 5 we find that for V_{latt} we have $A = 0.13900 \pm 0.00028, \alpha = 1.83090 \pm 0.00039$; for V_{na} we have $A = 0.28983 \pm 0.00042, \alpha = 1.92133 \pm 0.00028$; for V_{comb} we have $A = 0.093 \pm 9.0 \cdot 10^{-5}, \alpha = 1.9610 \pm 0.0050$; for V_{dw} we have $A = 0.94703 \pm 0.00054, \alpha = 1.97562 \pm 0.00011$. The fittings, as evident from Fig. 5 differ mainly by the prefactor, with losses for the V_{comb} being smaller with respect to the V_{latt} by approximately 30% for same value of U^{1111} . Together with order of magnitude larger J^1 potential V_{comb} provides a compelling way to realize a weakly interacting p -band superfluid.

When the offset of the subwavelength peak is introduced, for $\phi = 0.4/2\pi$ which maximizes the f -factor. The loss rate scaling is given by $A = 0.0863 \pm 0.0002, \alpha = 1.96956 \pm 0.00043$. This offers only marginal improvement over $\phi = 0$ case. As can be seen in Eqs. (22) and (23), while the factor f is increased from $1.94E_R$ to $3.38E_R$ the ratio of U^{1111}/U^{1120} is decreased from 9.02 down to 5.88. This means that for same U^{1111} the value of U^{1120} is actually larger in the $\phi \neq 0$ case. This consumes all benefits from increasing the f as f/U^{1102} is essentially the same in both cases.

IV. RESONANT COUPLING OF S-BAND TO P-BAND

A. Synthetic ladder

Coupling of the s and p bands can be achieved by a periodic modulation of the system with the frequency $\omega = \bar{E}^1 - \bar{E}^0$ (see [12–14, 19]). The other bands are off-resonant if $\omega = \bar{E}^1 - \bar{E}^2 \neq 0$ and in first approximation they can be neglected. We will study the degree to which neglecting other bands is possible for different potentials considered in this work.

The simplest coupling the bands s and p is by periodic modulation of the position of the lattice:

$$V(x, t) = V(x - A \sin \omega t).$$

The potential oscillation implies a co-movement of the instantaneous Wannier functions:

$$\mathcal{W}_n^\alpha(x, t) = \mathcal{W}_n^\alpha(x - A \sin \omega t)$$

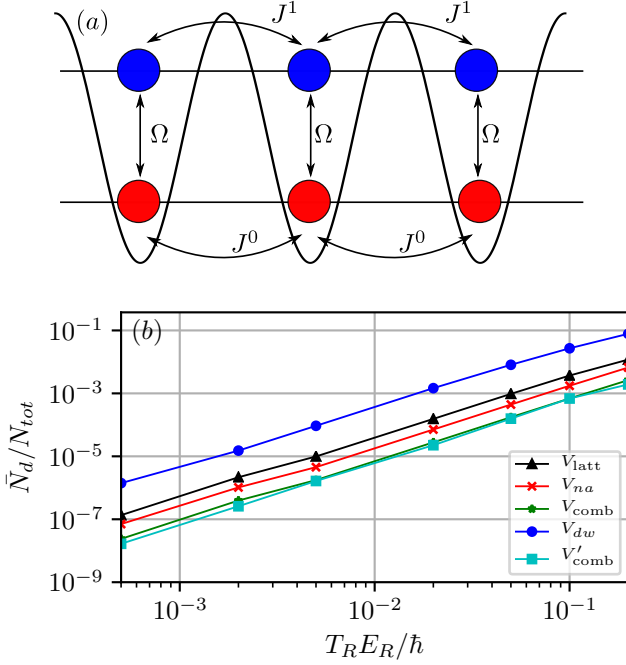


Figure 6. Mean losses from $s - p$ band, noninteracting ladder system measured as \bar{N}_d population as a function of T_R – Rabi frequency oscillation between s and p band (see text). Black triangles, red crosses, blue circles, green stars show losses for $V_{\text{latt}}, V_{na}, V_{dw}, V_{\text{comb}}$ lattices, for ($V_x = 30E_R, \epsilon = 0.1, V_1 = 20E_R, \phi = 0$ and $V_2 = 4E_R, V_1 = 20E_R$ and $\epsilon = 0.25$ respectively). The cyan V'_{comb} data series for configuration of V_{comb} but with $\phi = 0.4/2\pi$.

For fixed t the Hamiltonian (1), in the basis set by $\mathcal{W}_i^\alpha(x, t)$, will take the form of H_{MBH} with time-independent coefficients. Nevertheless, correctly derived time-evolution equation of motion, has to take into the account the time-dependence of the basis. The resulting Time dependent Schrödinger equation is of the form [14, 45]:

$$\partial_t \psi = H_{\text{MBH}} \psi - \sum_i \sum_{\alpha, \beta} [\mathcal{T}_{ii}^{\alpha\beta} A \omega \cos \omega t] (a_i^\alpha)^\dagger a_i^\beta \psi \quad (25)$$

The extra terms proportional to $\mathcal{T}_{nm}^{\alpha\beta}$ do not couple within the same band as $\forall m, n : \mathcal{T}_{nm}^{\alpha\alpha} = 0$. If the potential is symmetric with respect to the middle of the unit cell, the coefficients $\mathcal{T}_{ii}^{\alpha\beta} = 0, \alpha + \beta \equiv 0 \pmod{2}$, and they couple just bands of opposite parity, for example s and p band, but also e.g. p to the d band.

A 1D optical system, where population of bands other than s and p is precluded can be seen as a two leg ladder system [see Fig. 6(a)]. This shares many features with the synthetic dimension construction where in lieu of bands, different hyperfine states are used [46]. In particular, two sites at the ends of same ladder step, are physically in the same place, possibly allowing for strong interaction. The hoppings along the each of the lattice

legs is governed by J^0 and J^1 respectively, possibly allowing to implement complex ladder systems such as [33].

With no interaction, such an effective single particle system decomposes into fixed quasimomentum sectors:

$$i\hbar \partial_t \begin{pmatrix} \psi_k^0 \\ \psi_k^1 \end{pmatrix} = H_{\text{ladd}} \begin{pmatrix} \psi_k^0 \\ \psi_k^1 \end{pmatrix}, \quad (26)$$

where:

$$H_{\text{ladd}} = \begin{pmatrix} E^0(k) & iT^{01} A \omega \cos(\omega t) \\ -iT^{01} A \omega \cos(\omega t) & E^1(k) \end{pmatrix}. \quad (27)$$

By transforming to a rotating frame ($\psi_k^0 e^{i\delta_0 t}, \psi_k^1 e^{i\delta_1 t}$) and using the RWA, the equation of motion becomes time-independent, when $\delta_2 - \delta_1 = \omega$:

$$i\hbar \partial_t \begin{pmatrix} \psi_k^0 \\ \psi_k^1 \end{pmatrix} = H_{\text{ladd, RWA}} \begin{pmatrix} \psi_k^0 \\ \psi_k^1 \end{pmatrix}, \quad \Omega = T^{01} A \omega, \quad (28)$$

where

$$H_{\text{ladd, RWA}} = \begin{pmatrix} E^0(k) - \hbar\delta_0 & \Omega \\ \Omega & E^1(k) - \hbar\delta_1 \end{pmatrix}. \quad (29)$$

When $\delta_i \approx E^i(k)$, the Rabi oscillations frequency is $\Omega = T^{01} A \omega$. For Ω dominating the bandwidths ΔE^i this behavior is k -independent and Eq. (27) can be written as:

$$H_L = -J^0 \sum_{n=1}^L (a_n^0)^\dagger a_{n+1}^0 - J^1 \sum_{n=1}^L (a_n^1)^\dagger a_{n+1}^1 + H.d \quad (30)$$

$$+ iT_n^{01} A \omega (a_n^0)^\dagger a_n^1 \cos \omega t + H.c. + H_{\text{int.}}, \quad (31)$$

where

$$H_{L, \text{int}} = \sum_n \frac{U_{nnnn}^{\alpha\beta\gamma\delta}}{2} \sum_{\alpha, \beta, \gamma, \delta=0,1} (a_i^\alpha)^\dagger (a_i^\beta)^\dagger a_i^\gamma a_i^\delta. \quad (32)$$

When coupling to other bands beyond s and p cannot be neglected, system fails to be modeled by a two-leg ladder. This deviation from the ladder system is again measured by mean occupation of d and higher bands, $\delta = \bar{N}_{\geq d} / N_{\text{tot}}$. Depletion is possible also by means of the interaction.

B. Realization in different potentials

In this section we compare the implementations of Eq. (30) where the s and p bands are taken from the four discussed potentials. Specifically, the “perfect ladder” system is Eq. (25) truncated to the s, p bands. This leads to the desired Eq. (30). The closedness of such a system is compared to the model that also includes the d band, which is the most relevant band to consider in

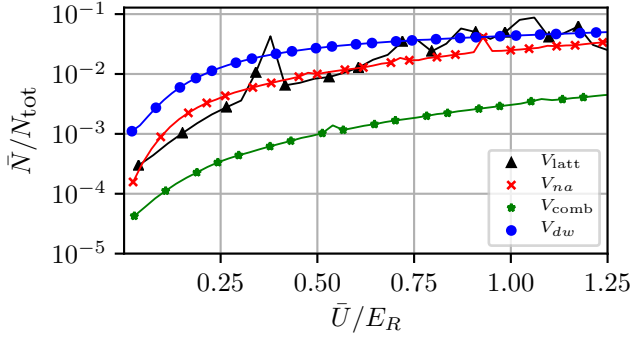


Figure 7. Depletion of the s, p band by as a function of $\bar{U} = (U^{0000} + U^{1111})/2$ for such an oscillation amplitude that corresponds to $T_R E_R / \hbar = 0.02$ in Fig. 6. At $\bar{U} = 0$ the depletion is finite and solely due to off-resonant coupling of s, p band to higher d band. Increase of the interaction results in further depletion of s, p band. The legend identifies the four potential discussed in the main text. The V_{comb} potential is characterized by losses smaller for large interaction approximately by an order of magnitude, despite much larger hopping values.

the study of couplings to other bands. Out of all bands beyond s, p the $\omega = \bar{E}^1 - \bar{E}^0$, for the class of potentials we consider, is closest to $\bar{E}^2 - \bar{E}^1$.

To meaningfully compare the four potentials we pick the same realizations in the Section III. In addition to parameter values given in Eqs. (20)-(24), we have that for $V_{\text{latt}}, V_{na}, V_{\text{comb}}, V_{dw}$ the $\mathcal{T}^{01} \approx 1.57E_R, 0.85E_R, 0.77E_R, 0.86E_R$ respectively. For the V_{comb} potential for $\phi = 0.4/2\pi$ we have $T^{01} \approx 1.36E_R$. It should be noted that in the latter case, due to lack of symmetry of the unit cell, also $T^{02} \approx 0.49E_R$.

We opt to compare the ladder depletion in the four potentials when all in all four cases the Rabi oscillation period T_R takes the same value. Ordinarily $T_R = 2\pi/\Omega$ with $\Omega = |\mathcal{T}^{01}A\omega|$. When coupling to the d band is included and becomes significant, the system does not undergo pure Rabi oscillation. More complicated oscillation pattern emerges. We define T_R for each amplitude of modulation by fitting the $A + B \sin(t/T_R)$ to the temporal dependence of $N_s(t)$.

First we consider a non-interacting ladder system of total length $L = 40$. We initialize the evolution with a quasi-momentum $k = 0$ state ψ_0 in the s -band. By fixing initial k allows consider Ω smaller than the bandwidth and still observe model Rabi oscillations, by setting $\omega = E^1(k = 0) - E^0(k = 0)$. As pictured in Fig. 6, the losses measured by \bar{N}_d , in the limit of small T_R scale as $\bar{N}_d = A(T_R)^c$. For the four potentials we find that : $\bar{N}_{d,\text{latt}} = (0.278 \pm 0.026)T_R^{1.909 \pm 0.020}$, $\bar{N}_{d,na} = (0.123 \pm 0.013)T_R^{1.899 \pm 0.022}$, $\bar{N}_{d,\text{comb}} = (0.0501 \pm 0.0053)T_R^{1.909 \pm 0.022}$, $\bar{N}_{d,dw} = (2.94 \pm 0.10)T_R^{1.9564 \pm 0.0071}$. For the alternative implementation of V_{comb} with $\phi = 0.4/2\pi$ we get $\bar{N}'_{d,\text{comb}} = (0.055 \pm 0.0031)T_R^{1.974 \pm 0.011}$. This scaling applies when $\bar{N}_d \ll 1$, In all cases we find

that $\bar{N}_{d,\text{comb}}$, are approximately an order of magnitude smaller than $\bar{N}_{d,\text{latt}}$, with $\bar{N}_{d,na}$, being in between. The losses for the double-well are order of magnitude larger than for the remaining systems. This is because of the lowest value of $f \approx 0.65E_R$ out of the four samples. The potential V_{comb} with $\phi = 0.4/2\pi$ again offers same stability as the $\phi = 0$. Nevertheless it features a strongly suppressed J^0 hopping along one of the lattice “legs” [as implied by Eq. (22) and Eq. (23)].

If the modulated system is also interacting an interesting interplay of shaking and interaction may occur. To simulate such a case we consider the same four potentials, modulated with a modulation amplitude A such that the noninteracting Rabi oscillation period $T_R = 0.02\hbar/E_R$. The length of the lattice is $L = 6$ with total $\rho L = 7$ particles.

The Fig. 7 shows the dependence of the \bar{N}_d on the mean interaction strength $\bar{U} = (U^{0000} + U^{1111})/2$ (see also (20)-(24)). The interaction strength would be tuned with use of the Feshbach resonance, thus scaling both U^{1111}, U^{0000} by a common factor. For $\bar{U} = 0$ the results from Fig. 7 are reproduced. For increasing $\bar{U} > 0$ for each of the four potentials the interaction causes the additional losses on top of the modulation losses. It is evident that the losses for the V_{comb} potential grow slowest with the \bar{U} [here again losses for $\phi = 0$ are essentially the same as for $\phi = 0.4/2\pi$]. This is due to the combination of factors: first it allows to reach high anharmonic band placement (large value of $f \approx 2E_R$), second as evident from Fig. 4 the value of $|U^{1102}/\bar{U}|$ is relatively small compared to other potentials 0.17, 0.32, 0.11, 0.23 for $V_{\text{latt}}, V_{na}, V_{\text{comb}}, V_{dw}$ (for V_{comb} for $\phi = 0.4/2\pi$ we have $|U^{1102}/\bar{U}| \approx 0.105$). This means that if \bar{U} is fixed to a given value, then the terms responsible for interaction-driven losses come with a smaller prefactor than in the other potentials. This advantage together with largest value of f (which affects also modulation) allows to observe order of magnitude smaller depletion of the s, p band system. This also explains the difference in stability for $\bar{U} \neq 0$.

V. CONCLUSIONS AND OUTLOOKS

The subwavelength comb potential makes it possible to implement potentials that break the constraints implied by the diffraction limit put on constructions based on the AC-Stark effects. We have constructed lattice potentials with anharmonic potential wells, that can be realistically implemented in laboratory. The anharmonicity enhances the collisional stability of the p -band gas. Moreover, the s and p bands of the lattice can be resonantly coupled by modulation, and the resulting couplings from s, p bands to other bands can be sufficiently off-resonant to neglect them for even stronger coupling strength than the standard lattice. The latter was presented by implementing a synthetic dimension $s - p$ band ladder.

Another important feature of the constructed poten-

tials is the ability to preserve large value of the hopping rate. They offer controllable work with the p band in the regime of large hopping amplitude.

The remaining open question is the applicability of the construction for the interacting bosonic systems. A fundamental problem is description of interaction-driven depletion of dark states, and a choice of a proper atom species that would allow the Λ system construction in

for an collisionally interacting ultracold atom gas.

ACKNOWLEDGMENTS

This work has been supported by National Science Centre project 2016/23/D/ST2/00721 and in part by PL-Grid Infrastructure (prometheus cluster).

-
- [1] D. Jaksch, C. Bruder, J. I. Cirac, C. W. Gardiner, and P. Zoller, *Physical Review Letters* **81**, 3108 (1998).
 - [2] M. Greiner, O. Mandel, T. Esslinger, T. W. Hänsch, and I. Bloch, *nature* **415**, 39 (2002).
 - [3] M. Lewenstein, A. Sanpera, and V. Ahufinger, *Ultracold Atoms in Optical Lattices: Simulating quantum many-body systems* (Oxford University Press, 2012).
 - [4] T. Müller, S. Fölling, A. Widera, and I. Bloch, *Physical review letters* **99**, 200405 (2007).
 - [5] G. Wirth, M. Ölschläger, and A. Hemmerich, *Nature Physics* **7**, 147 (2011).
 - [6] X. Li, Z. Zhang, and W. V. Liu, *Physical review letters* **108**, 175302 (2012).
 - [7] T. Sowiński, M. Łacki, O. Dutta, J. Pietraszewicz, P. Sierant, M. Gajda, J. Zakrzewski, and M. Lewenstein, *Physical review letters* **111**, 215302 (2013).
 - [8] P. Hauke, E. Zhao, K. Goyal, I. H. Deutsch, W. V. Liu, and M. Lewenstein, *Physical Review A* **84**, 051603 (2011).
 - [9] M. Ölschläger, T. Kock, G. Wirth, A. Ewerbeck, C. M. Smith, and A. Hemmerich, *New Journal of Physics* **15**, 083041 (2013).
 - [10] C. Wu, *Physical review letters* **101**, 186807 (2008).
 - [11] M. Zhang, H.-h. Hung, C. Zhang, and C. Wu, *Physical Review A* **83**, 023615 (2011).
 - [12] N. Gemelke, E. Sarajlic, Y. Bidel, S. Hong, and S. Chu, *Physical review letters* **95**, 170404 (2005).
 - [13] T. Sowiński, *Physical review letters* **108**, 165301 (2012).
 - [14] M. Łacki and J. Zakrzewski, *Physical review letters* **110**, 065301 (2013).
 - [15] X. Zhou, S. Jin, and J. Schmiedmayer, *New Journal of Physics* **20**, 055005 (2018).
 - [16] M. Köhl, H. Moritz, T. Stöferle, K. Günter, and T. Esslinger, *Physical review letters* **94**, 080403 (2005).
 - [17] D. Hu, L. Niu, B. Yang, X. Chen, B. Wu, H. Xiong, and X. Zhou, *Physical Review A* **92**, 043614 (2015).
 - [18] L. Niu, S. Jin, X. Chen, X. Li, and X. Zhou, *Physical review letters* **121**, 265301 (2018).
 - [19] C. Cabrera-Gutiérrez, E. Michon, M. Arnal, G. Chatelain, V. Brunaud, T. Kawalec, J. Billy, and D. Guéry-Odelin, *The European Physical Journal D* **73**, 170 (2019).
 - [20] C. Sträter and A. Eckardt, *Physical Review A* **91**, 053602 (2015).
 - [21] A. Kastberg, W. D. Phillips, S. Rolston, R. Spreuw, and P. S. Jessen, *Physical review letters* **74**, 1542 (1995).
 - [22] A. Isacsson and S. Girvin, *Physical Review A* **72**, 053604 (2005).
 - [23] M. Łacki, M. Baranov, H. Pichler, and P. Zoller, *Physical review letters* **117**, 233001 (2016).
 - [24] Y. Wang, S. Subhankar, P. Bienias, M. Łacki, T.-C. Tsui, M. A. Baranov, A. V. Gorshkov, P. Zoller, J. V. Porto, S. L. Rolston, *et al.*, *Physical review letters* **120**, 083601 (2018).
 - [25] J. Budich, A. Elben, M. Łacki, A. Sterdyniak, M. Baranov, and P. Zoller, *Physical Review A* **95**, 043632 (2017).
 - [26] C. Chin, R. Grimm, P. Julienne, and E. Tiesinga, *Reviews of Modern Physics* **82**, 1225 (2010).
 - [27] W. Kohn, *Physical Review* **115**, 809 (1959).
 - [28] S. Kivelson, *Physical Review B* **26**, 4269 (1982).
 - [29] N. Marzari, A. A. Mostofi, J. R. Yates, I. Souza, and D. Vanderbilt, *Reviews of Modern Physics* **84**, 1419 (2012).
 - [30] M. P. Fisher, P. B. Weichman, G. Grinstein, and D. S. Fisher, *Physical Review B* **40**, 546 (1989).
 - [31] T. Stöferle, H. Moritz, C. Schori, M. Köhl, and T. Esslinger, *Physical review letters* **92**, 130403 (2004).
 - [32] J. Zakrzewski and D. Delande, in *AIP Conference Proceedings*, Vol. 1076 (American Institute of Physics, 2008) pp. 292–300.
 - [33] X. Li, E. Zhao, and W. V. Liu, *Physical Review A* **83**, 063626 (2011).
 - [34] M. Mark, E. Haller, K. Lauber, J. Danzl, A. Daley, and H.-C. Nägerl, *Physical review letters* **107**, 175301 (2011).
 - [35] M. Lacki, P. Zoller, and M. Baranov, *Physical Review A* **100**, 033610 (2019).
 - [36] V. Boyer, R. Godun, G. Smirne, D. Cassettari, C. Chandrashekar, A. Deb, Z. Laczik, and C. Foot, *Physical Review A* **73**, 031402 (2006).
 - [37] J. Liang, R. N. Kohn Jr, M. F. Becker, and D. J. Heinzen, *Applied optics* **49**, 1323 (2010).
 - [38] D. Bowman, P. Ireland, G. D. Bruce, and D. Cassettari, *Optics Express* **23**, 8365 (2015).
 - [39] J. Sebby-Strabley, M. Anderlini, P. S. Jessen, and J. V. Porto, *Physical Review A* **73**, 033605 (2006).
 - [40] M. Anderlini, J. Sebby-Strabley, J. Kruse, J. V. Porto, and W. D. Phillips, *Journal of Physics B: Atomic, Molecular and Optical Physics* **39**, S199 (2006).
 - [41] V. M. Stojanović, C. Wu, W. V. Liu, and S. D. Sarma, *Physical review letters* **101**, 125301 (2008).
 - [42] P. Lee, M. Anderlini, B. Brown, J. Sebby-Strabley, W. Phillips, and J. Porto, *Physical Review Letters* **99**, 020402 (2007).
 - [43] M. Anderlini, P. J. Lee, B. L. Brown, J. Sebby-Strabley, W. D. Phillips, and J. V. Porto, *Nature* **448**, 452 (2007).
 - [44] T.-C. Tsui, Y. Wang, S. Subhankar, J. V. Porto, and S. L. Rolston, (2019), arXiv:1911.00394 [cond-mat.quant-gas].
 - [45] H. Pichler, J. Schachenmayer, A. J. Daley, and P. Zoller, *Physical Review A* **87**, 033606 (2013).
 - [46] A. Celi, P. Massignan, J. Ruseckas, N. Goldman, I. B. Spielman, G. Juzeliūnas, and M. Lewenstein, *Physical review letters* **112**, 043001 (2014).